Electronic Supplementary Information

In situ construction and post-electrolysis structural study of porous Ni_2P@C nanosheet arrays for efficient water splitting

Min Ma,[a] Zhiping Zheng,[a] Zhijia Song,[a] Xibo Zhang,[a] Xiao Han,[a] Hanming Chen,[a] Zhaoxiong Xie,[a,b] Qin Kuang,[a*] and Lansun Zheng[a]

[a] State Key Laboratory of Physical Chemistry of Solid Surfaces & Department of Chemistry, College of Chemistry and Chemical Engineering, Xiamen University, Xiamen 361005, Fujian (P. R. China). E-mail: qkuang@xmu.edu.cn; Fax: (+) 86-592-2183047.

[b] Pen-Tung Sah Institute of Micro-Nano Science and Technology, Xiamen University, Xiamen 361005, Fujian (P. R. China).

1. Experimental Section

Materials: Nickel chloride hexahydrate ($NiCl_2 \cdot 6H_2O$), sodium hypophosphite hydrate ($NaH_2PO_2 \cdot H_2O$), ammonium fluoride (NH_4F), hexamethylenetetramine (HMT), hydrochloric acid (HCl), N,N-dimethylformamide (DMF), and ethanol (C_2H_5OH) were purchased from Sinopharm Chemical Reagent Co. Ltd. (Shanghai, China). Terephthalic acid ($C_8H_6O_4$) was purchased from Energy Chemical (Shanghai, China). Nafion (5 wt%) was supplied by Sigma-Aldrich Chemical Reagent Co., Ltd. Pt/C (10 wt%) was provided by Alfa Aesar (China) Chemicals Co., Ltd., while RuO_2 was supplied by Aladdin Ltd. (Shanghai, China). NF was purchased from Shenzhen Green and Creative Environmental Science and Technology Co., Ltd. All chemical regents were used as received without further purification (except NF). Ultrapure water was used throughout all experiments.

Preparation of RuO_2 and Pt/C working electrodes: 5 mg of RuO_2 (or Pt/C) were dispersed in a solution containing 500 μL C_2H_5OH, 480 μL water, and 20 μL Nafion. Subsequently, the above solution was ultrasonicated for 1 h to obtain a uniform ink. The resulting ink (400 μL) was then carefully coated on a cleaned NF (1×1 cm^2), and the NF with a catalyst loading (RuO_2 or Pt/C) of 2 mg cm^{-2} was dried at 60 °C for 2 h. The Ni_2P@C powder working electrode was also prepared using the above procedure.

Characterizations: XRD measurements were performed using a Rigaku Ultima IV diffractometer with Cu Kα radiation (40 KV, 30 mA). SEM images of our samples were collected on a Hitachi S4800 SEM at an accelerating voltage of 15 kV. XPS data were recorded on an ESCALab 250 X-ray photoelectron spectrometer using non-monochromatic Al Kα X-rays as the excitation source. TEM measurements were performed on a JEOL2100 TEM with an accelerating voltage of 200 kV. HAADF-STEM, EDX data, and elemental mapping images were recorded on an FEI TECNAI F30 microscope at 300 KV. Raman spectra were collected on a confocal microscope (XploRA INV HORIBA) using a 638 nm laser beam at ambient temperature.

2. Supplementary Results

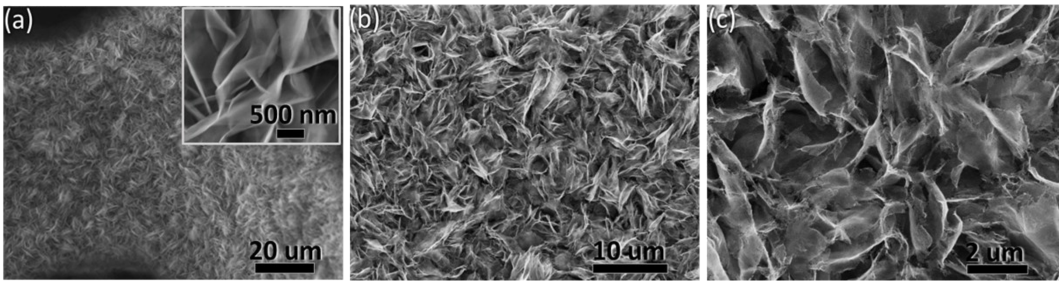

Fig. S1. SEM images of (a) NiMOF NAs/NF and (b-c) $Ni_2P@C$ NAs/NF at different magnifications.

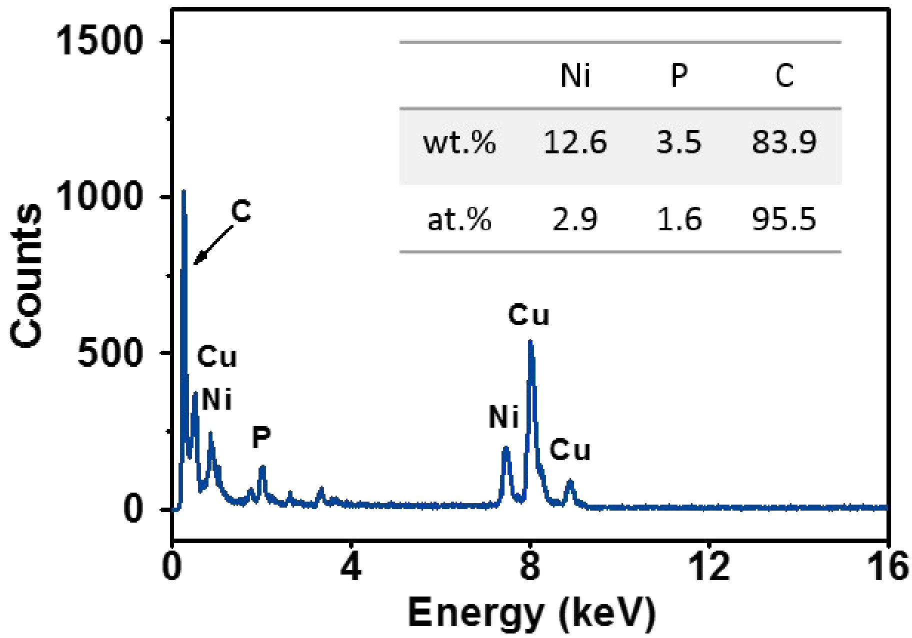

Fig. S2 EDX spectrum of $Ni_2P@C$ NAs/NF.

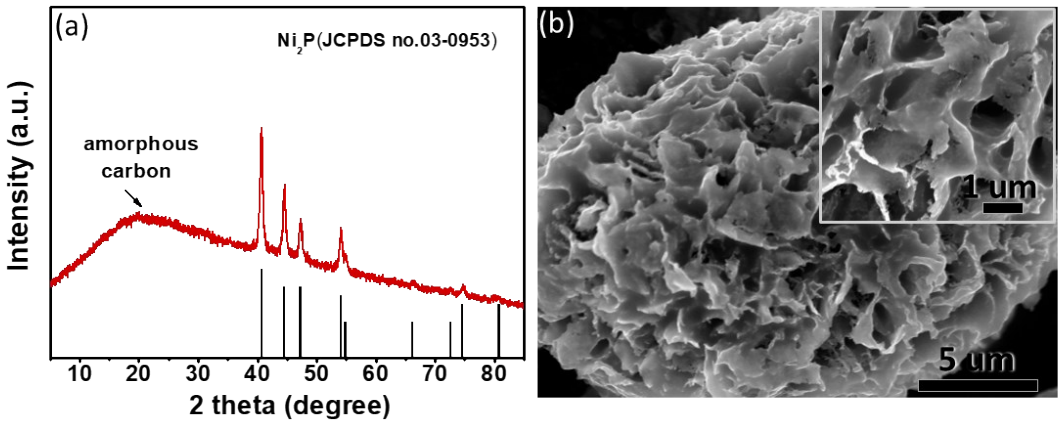

Fig. S3 (a) XRD pattern and (b) SEM images of Ni_2P@C powder.

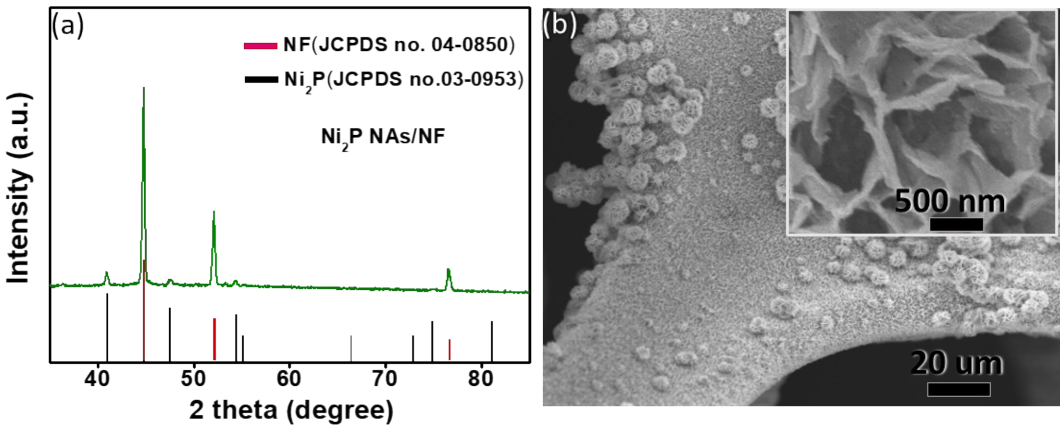

Fig. S4 (a) XRD pattern and (b) SEM images of Ni_2P NAs/NF.

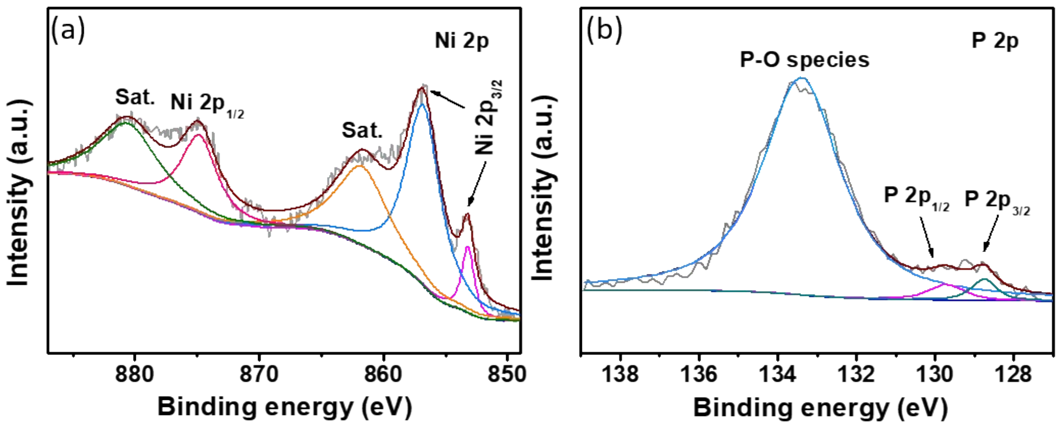

Fig. S5 High-resolution XPS spectra for Ni_2P NAs/NF in the (a) Ni 2p and (b) P 2p regions.

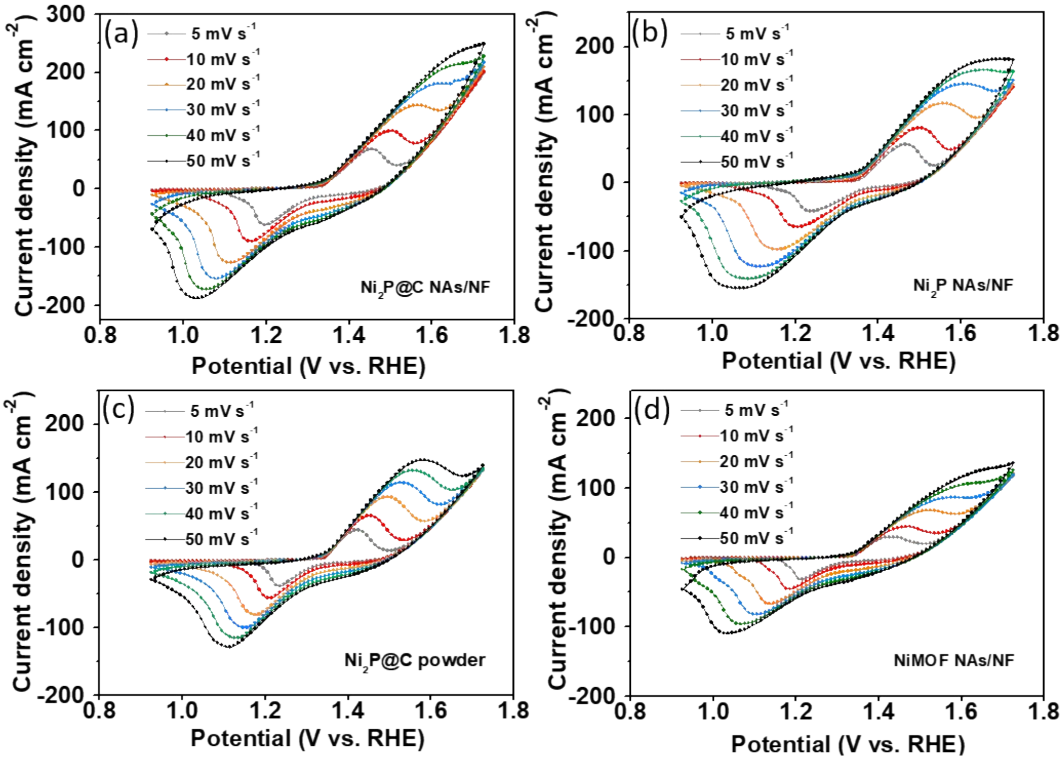

Fig. S6 CV curves recorded for (a) Ni_2P@C NAs/NF, (b) Ni_2P NAs/NF, (c) Ni_2P@C powder, and (d) NiMOF NAs/NF at different scanning rates from 5 to 50 mV s^{-1} tested in 1.0 M KOH.

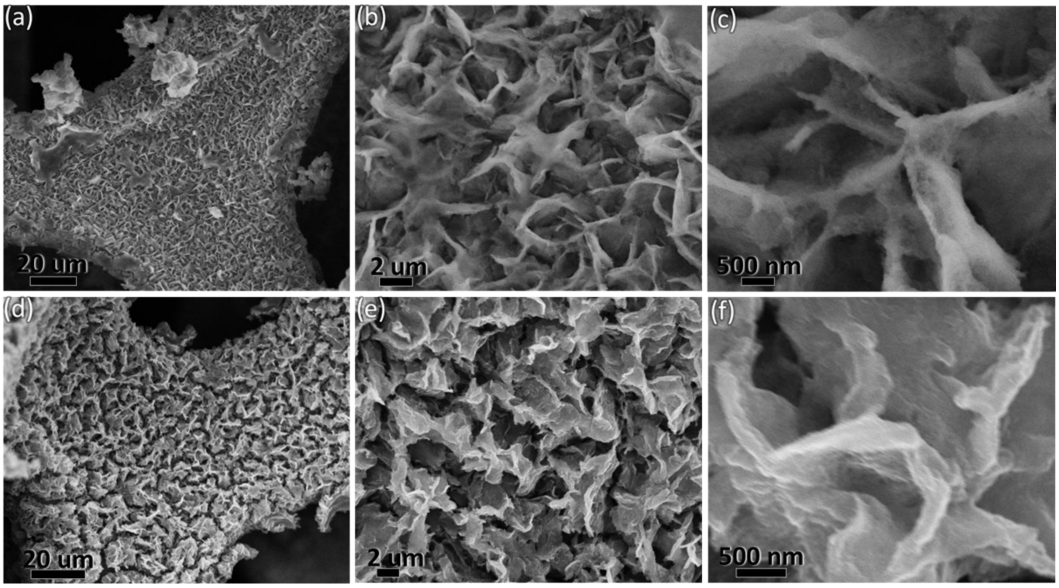

Fig. S7 SEM images under different magnifications of (a-c) cathodic and (d-f) anodic Ni_2P@C NAs/NF after water electrolysis for 36 h.

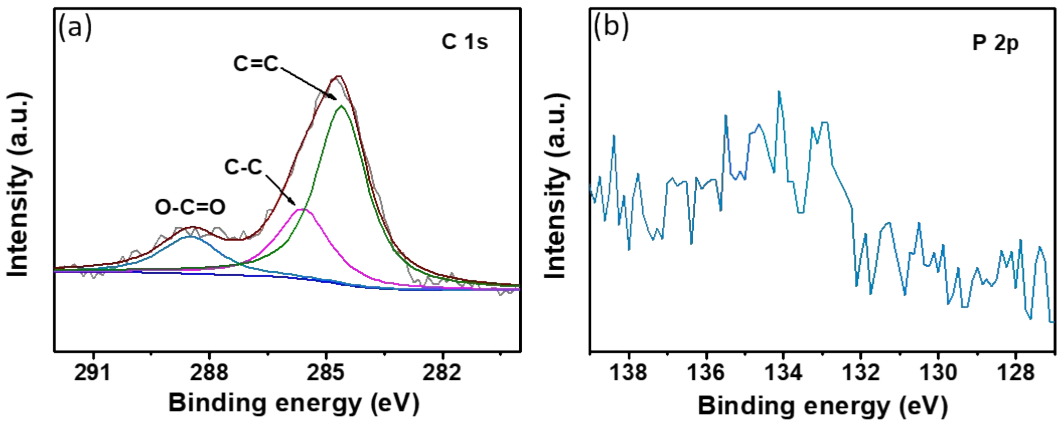

Fig. S8 High-resolution XPS spectra for post-electrolysis Ni_2P@C NAs/NF in the (a) C 1s and (b) P 2p regions.

Table S1. Comparisons of OER performance for Ni_2P@C NAs/NF with other noble metal-free based catalyst materials operated in alkaline electrolyte. It should be stated that the extracted overpotential (η) was required to deliver a catalytic current density of 10 mA cm^{-2} except an especial illustration.

Catalyst	Overpotential η_{10} (mV)	Tafel slope (mV dec^{-1})	Electrolyte	Ref.
Ni_2P@C NAs/NF	$243_{15\ mA\ cm\text{-}2}$	58	1.0 M KOH	This work
	$280_{50\ mA\ cm\text{-}2}$			
	$297_{100\ mA\ cm\text{-}2}$			
CoP/NCNHP	310	70	1.0 M KOH	[1]
NiCo LDH nanoleaf	262	49.36	1.0 M KOH	[2]
Ni_2P/CoN–PCP	270	65	0.1 M KOH	[3]
CoOx@CN hybrids	260	~	1.0 M KOH	[4]
MOF-derived Ni_2P–CoP	320	69	0.1 M KOH	[5]
NGO/Ni_7S_6	380	45.4	0.1 M KOH	[6]
Porous Ni_2P nanosheets	320	105	1.0 M KOH	[7]
CNTs@NiCoP/C	297	57.35	1.0 M KOH	[8]
Ni_2P–Ni_3S_2 HNAs/NF	210	62	1.0 M KOH	[9]
Ni_3S_2/NF	260	~	1.0 M KOH	[10]
Nickel-iron oxide/C	310	42	1.0 M KOH	[11]
$Ni_{45}Fe_{55}$ oxyhydroxide	310	65	0.1 M KOH	[12]
NiCoP/C	330	96	1.0 M KOH	[13]
NiS/Ni_2P/CC	$265_{20\ mA\ cm\text{-}2}$	41.3	1.0 M KOH	[14]
Ni_5P_4 films	$270_{20\ mA\ cm\text{-}2}$	ca. 40	1.0 M KOH	[15]
Ni–P/CF	325	120	1.0 M KOH	[16]
CoP/rGO	340	66	1.0 M KOH	[17]
FeP/Ni_2P hollow nanospindles	234	56	1.0 M KOH	[18]
$NiSe_2$–Ni_2P/NF	$220_{50\ mA\ cm\text{-}2}$	45	1.0 M KOH	[19]
Ni/Ni_2P@3DNSC	231	67	1.0 M KOH	[20]
Ni_3FeN-NPs	280	46	1.0 M KOH	[21]

Co–P films	345	47	1.0 M KOH	[22]
NiCo LDH	367	40	1.0 M KOH	[23]
Ni_3Se_2–GC	310	97.1	1.0 M KOH	[24]
Cu_3P microsheets	290	84	1.0 M KOH	[25]
Co/CoP nanoparticles	340	79.5	1.0 M KOH	[26]
Fe doped CoP nanoarray	230	67	1.0 M KOH	[27]
Ni_2P hollow microspheres	270	40.4	1.0 M KOH	[28]
FeB_2 nanoparticles	296	52.4	1.0 M KOH	[29]
CP/CTs/Co–S	306	72	1.0 M KOH	[30]
NiSe/NF	$270_{20\ \mathrm{mA\ cm^{-2}}}$	64	1.0 M KOH	[31]
Ternary NiCoP nanosheet arrays	$308_{50\ \mathrm{mA\ cm^{-2}}}$	68.6	1.0 M KOH	[32]
$NiCo_2S_4$ NA/CC	$340_{100\ \mathrm{mA\ cm^{-2}}}$	89	1.0 M KOH	[33]
ECT-$Co_{0.37}Ni_{0.26}Fe_{0.37}O$	232	37.6	1.0 M KOH	[34]
C@Ni_8P_3	267	51	1.0 M KOH	[35]
Ni_2P particles	290	59	1.0 M KOH	[36]
$NiCo_2O_4$	ca. $480_{100\ \mathrm{mA\ cm^{-2}}}$	60	1.0 M KOH	[37]
CoMnP	330	61	1.0 M KOH	[38]
Co_3O_4C-NA	290	70	0.1 M KOH	[39]
BP/Co_2P	ca. 380	78	1.0 M KOH	[40]

Table S2. R_s, R_{ct1}, R_{ct2} values of different catalyst electrodes in the equivalent circuit model.

Catalyst	R_s	R_{ct1}	R_{ct2}
Ni_2P@C NAs/NF	1.61	2.03	0.52
Ni_2P NAs/NF	1.68	2.16	0.40
Ni_2P@C powder	1.63	2.58	0.52
NiMOF NAs/NF	1.60	4.92	0.28

Table S3. Comparisons of HER performance for Ni_2P@C NAs/NF with other noble metal-free based electrocatalysts. It should be stated that the overpotential (η) recorded in this table was required to afford a current density of 10 mA cm^{-2} except especially explained.

Catalyst	Overpotential η_{10} (mV)	Tafel slope (mV dec^{-1})	Electrolyte	Ref.
Ni_2P@C NAs/NF	122	102	1.0 M KOH	This work
CoP/NCNHP	140	53	1.0 M KOH	[1]
CoOx@CN hybrids	232	115	1.0 M KOH	[4]
MOF-derived Ni_2P–CoP	105	64	0.5 M H_2SO_4	[5]
NGO/Ni_7S_6	37	145.5	0.1 M KOH	[6]
Porous Ni_2P nanosheets	168	63	1.0 M KOH	[7]
Ni_2P–Ni_3S_2 HNAs/NF	80	65	1.0 M KOH	[9]
Ni_3S_2/NF	223	~	1.0 M KOH	[10]
NiS/Ni_2P/CC	$111_{20\ mA\ cm-2}$	78.1	1.0 M KOH	[14]
Ni_5P_4 films	$190_{20\ mA\ cm-2}$	53	1.0 M KOH	[15]
Ni–P/CF	98	55	1.0 M KOH	[16]
CoP/rGO	150	38	1.0 M KOH	[17]
Ni/Ni_2P@3DNSC	92	65	1.0 M KOH	[20]
Ni_3FeN-NPs	158	42	1.0 M KOH	[21]
Co–P films	94	42	1.0 M KOH	[22]
Cu_3P microsheets	130	83	1.0 M KOH	[25]
Co/CoP nanoparticles	253	73.8	1.0 M KOH	[26]
Fe doped CoP nanoarray	78	60	1.0 M KOH	[27]
Ni_2P hollow microspheres	100	86.4	1.0 M KOH	[28]
CP/CTs/Co–S	190	131	1.0 M KOH	[30]
NiSe/NF	96	120	1.0 M KOH	[31]
Ni_2P particles	ca. 220	~	1.0 M KOH	[36]
CoP/Co-MOF hybrid	34	56	1.0 M KOH	[41]
Ni_2P−Cu_3P@NiCuC	78	173	1.0 M KOH	[42]

Table S4. Comparisons of water-splitting activity for two-electrode electrolyzer assembled by Ni_2P@C NAs/NF with those electrolyzers based on previous non-noble metal based electrocatalysts. It should be stated that the cell voltage recorded in this table was applied at a water-splitting current of 10 mA cm^{-2} except especially explained.

Catalyst	Applied voltage at 10 mA cm^{-2}	Electrolyte	Ref.
Ni_2P@C NAs/NF	1.64 V	1.0 M KOH	This work
CoP/NCNHP	1.64 V	1.0 M KOH	[1]
CoOx@CN hybrids	1.55 $V_{20\ mA\ cm-2}$	0.1 M KOH	[4]
Ni_2P–Ni_3S_2 HNAs/NF	1.50	1.0 M KOH	[9]
Ni_3S_2/NF	1.70	1.0 M KOH	[10]
NiS/Ni_2P/CC	1.67	1.0 M KOH	[14]
Ni_5P_4 films	1.68	1.0 M KOH	[15]
Ni–P/CF	1.68	1.0 M KOH	[16]
CoP/rGO	1.70	1.0 M KOH	[17]
Ni/Ni_2P@3DNSC	1.55	1.0 M KOH	[20]
Co–P films	$1.74_{100\ mA\ cm-2}$	1.0 M KOH	[22]
Fe doped CoP nanoarray	1.60	1.0 M KOH	[27]
Ni_2P hollow microspheres	$1.64_{20\ mA\ cm-2}$	1.0 M KOH	[28]
CP/CTs/Co–S	ca. 1.74	1.0 M KOH	[30]
NiSe/NF	1.63	1.0 M KOH	[31]
Ni_2P particles	1.63	1.0 M KOH	[36]
β-$Ni(OH)_2$/$NiSe_2$ couple	1.78	1.0 M KOH	[43]
$CoNi(OH)_x$/NiN_x couple	1.64	1.0 M KOH	[44]
NiFe/$NiCo_2O_4$/NF	1.67	1.0 M KOH	[45]
Fe-Ni@NC-CNTs	ca. 1.72	1.0 M KOH	[46]
$Ni_{11}(HPO_3)_8(OH)_6$	1.6	1.0 M KOH	[47]
NF@Ni/C-600	$1.60_{35.9\ mA\ cm-2}$	1.0 M KOH	[48]

References

[1] Y. Pan, K. Sun, S. Liu, X. Cao, K. Wu, W.-C. Cheong, Z. Chen, Y. Wang, Y. Li, Y. Liu, D. Wang, Q. Peng, C. Chen, Y. Li, Core-shell ZIF-8@ZIF-67-derived CoP nanoparticle-embedded N-doped carbon nanotube hollow polyhedron for efficient overall water splitting, *J. Am. Chem. Soc.,* 2018*,* **140***,* 2610−2618.

[2] B. Chen, Z. Zhang, S. Kim, M. Baek, D. Kim, K. Yong, A biomimetic nanoleaf electrocatalyst for robust oxygen evolution reaction, *Appl. Catal. B,* 2019, **259**, 118017.

[3] T. Sun, S. Zhang, L. Xu, D. Wang, Y. Li, An efficient multifunctional hybrid electrocatalyst: Ni_2P nanoparticles on MOF-derived Co,N-doped porous carbon polyhedrons for oxygen reduction and water splitting, *Chem. Commun.,* 2018, **54**, 12101−12104.

[4] H. Jin, J. Wang, D. Su, Z. Wei, Z. Pang, Y. Wang, C and N hybrid coordination derived Co-C-N complex as a highly efficient electrocatalyst for hydrogen evolution reaction, *J. Am. Chem. Soc.,* 2015, **137**, 2688−2694.

[5] X. Liang, B. Zheng, L. Chen, J. Zhang, Z. Zhuang, B.-H. Chen, MOF-derived formation of Ni_2P-CoP bimetallic phosphides with strong interfacial effect toward electrocatalytic water splitting, *ACS Appl. Mater. Interfaces,* 2017, **9**, 23222−23229.

[6] K. Jayaramulu, J. Masa, O. Tomanec, D. Peeters, V. Ranc, A. Schneemann, R. Zboril, W. Schuhmann, R. A. Fischer, Nanoporous nitrogen-doped graphene oxide/nickel sulfide composite sheets derived from a metal-organic framework as

an efficient electrocatalyst for hydrogen and oxygen evolution, *Adv. Funct. Mater.,* 2017, **27**, 1700451.

[7] Q. Wang, Z. Liu, H. Zhao, H. Huang, H. Jiao, Y. Du, MOF-derived porous Ni_2P nanosheets as novel bifunctional electrocatalysts for the hydrogen and oxygen evolution reactions, *J. Mater. Chem. A,* 2018, **6**, 18720−18727.

[8] Y. Zhao, G. Fan, L. Yang, Y. Lin, F. Li, Assembling Ni-Co phosphides/carbon hollow nanocages and nanosheets with carbon nanotubes into a hierarchical necklace-like nanohybrid for electrocatalytic oxygen evolution reaction, *Nanoscale,* 2018, **10**, 13555–13564.

[9] L. Zeng, K. Sun, X. Wang, Y. Liu, Y. Pan, Z. Liu, D. Cao, Y. Song, S. Liu, C. Liu, Three-dimensional-networked Ni_2P/Ni_3S_2 heteronanoflake arrays for highly enhanced electrochemical overall-water-splitting activity, *Nano Energy,* 2018, **51**, 26–36.

[10] L. L. Feng, G. Yu, Y. Wu, G. D. Li, H. Li, Y. Sun, T. Asefa, W. Chen, X. Zou, High-index faceted Ni_3S_2 nanosheet arrays as highly active and ultrastable electrocatalysts for water splitting, *J Am. Chem. Soc.,* 2015, **137**, 14023–14026.

[11] P. Li, Z. Jin, J. Yang, Y. Jin, D. Xiao, Highly active 3D-nanoarray-supported oxygen-evolving electrode generated from cobalt-phytate nanoplates, *Chem. Mater.,* 2016, **28**, 153–161.

[12] M. Goerlin, P. Chernev, J. F. de Araujo, T. Reier, S. Dresp, B. Paul, R. Kraehnert, H. Dau, P. Strasser, Oxygen evolution reaction dynamics, faradaic charge

efficiency, and the active metal redox states of Ni-Fe oxide water splitting electrocatalysts, *J Am. Chem. Soc.,* 2016, **138**, 5603–5614.

[13] P. He, X.-Y. Yu, X. W. Lou, Carbon-incorporated nickel-cobalt mixed metal phosphide nanoboxes with enhanced electrocatalytic activity for oxygen evolution, *Angew. Chem., Int. Ed.,* 2017, **56**, 3897–3900.

[14] X. Xiao, D. Huang, Y. Fu, M. Wen, X. Jiang, X. Lv, M. Li, L. Gao, S. Liu, M. Wang, C. Zhao, Y. Shen, Engineering NiS/Ni_2P heterostructures for efficient electrocatalytic water splitting, *ACS Appl. Mater. Interfaces,* 2018, **10**, 4689−4696.

[15] M. Ledendecker, S. K. Calderýn, C. Papp, H.-P. Steinrîck, M. Antonietti, M. Shalom, The synthesis of nanostructured Ni_5P_4 films and their use as a non-noble bifunctional electrocatalyst for full water splitting, *Angew. Chem., Int. Ed.,* 2015, **54**, 12361–12365.

[16] Q. Liu, S. Gu, C. M. Li, Electrodeposition of nickel-phosphorus nanoparticles film as a Janus electrocatalyst for electro-splitting of water, *J. Power Sources,* 2015, **299**, 342–346.

[17] L. Jiao, Y.-X. Zhou, H.-L. Jiang, Metal-organic framework-based CoP/reduced graphene oxide: high-performance bifunctional electrocatalyst for overall water splitting, *Chem. Sci.,* 2016, **7**, 1690–1695.

[18] Y. Feng, C. Xu, E. Hu, B. Xia, J. Ning, C. Zheng,Y. Zhong, Z. Zhang, Y. Hu, Construction of hierarchical FeP/Ni_2P hollow nanospindles for efficient oxygen evolution, *J. Mater. Chem. A,* 2018, **6**, 14103–14111.

[19] P. Wang, Z. Pu, W. Li, J, Zhu, C, Zhang, Y. Zhao, S. Mu, Coupling $NiSe_2$-Ni_2P heterostructure nanowrinkles for highly efficient overall water splitting, *J. Catal.,* 2019, **377**, 600–608.

[20] Y. Sun, T. Zhang, X. Li, Y. Bai, X. Lyu, G. Liu, W. Cai, Y. Li, Bifunctional hybrid Ni/Ni_2P nanoparticles encapsulated by graphitic carbon supported with N,S modified 3D carbon framework for highly efficient overall water splitting, *Adv. Mater. Interfaces,* 2018, **5**, 1800473.

[21] X. Jia Y. Zhao G. Chen, L. Shang , R. Shi, X. Kang, G. I. N. Waterhouse, L.-Z. Wu, C.-H. Tung, T. Zhang, Ni_3FeN nanoparticles derived from ultrathin NiFe-layered double hydroxide nanosheets: an efficient overall water splitting electrocatalyst, *Adv. Energy. Mater.,* 2016*,* **6***,* 1502585.

[22] N. Jiang, B. You, M. Sheng, Y. Sun, Electrodeposited cobalt-phosphorous-derived films as competent bifunctional catalysts for overall water splitting, *Angew. Chem., Int. Ed.,* 2015, **54**, 6251−6254.

[23] H. Liang, F. Meng, M. Caban-Acevedo, L. Li, A. Forticaux, L. Xiu, Z. Wang, S. Jin, Hydrothermal continuous flow synthesis and exfoliation of NiCo layered double hydroxide nanosheets for enhanced oxygen evolution catalysis, *Nano Lett.,* 2015, **15**, 1421−1427.

[24] A. T. Swesi, J. Masud, M. Nath, Nickel selenide as a high-efficiency catalyst for oxygen evolution reaction, *Energy Environ. Sci.,* 2016, **9**, 1771−1782.

[25] J. Hao, W. Yang, Z. Huang, C. Zhang, Superhydrophilic and superaerophobic copper phosphide microsheets for efficient electrocatalytic hydrogen and oxygen evolution, *Adv. Mater. Interfaces,* 2016, **3**, 1600236.

[26] Z.-H. Xue, H. Su, Q.-Y. Yu, B. Zhang, H.-H. Wang, X.-H. Li, J.-S. Chen, Janus Co/CoP nanoparticles as efficient Mott-Schottky electrocatalysts for overall water Splitting in wide pH range, *Adv. Energy. Mater.,* 2017, **7**, 1602355.

[27] C. Tang, R. Zhang, W. Lu, L. He, X. Jiang, A. M. Asiri, X. Sun, Fe-doped CoP nanoarray: a monolithic multifunctional catalyst for highly efficient hydrogen generation, *Adv. Mater.,* 2017, **29**, 1602441.

[28] H. Sun, X. Xu, Z. Yan, X. Chen, F. Cheng, P. S. Weiss, J. Chen, Porous multishelled Ni_2P hollow microspheres as an active electrocatalyst for hydrogen and oxygen evolution, *Chem. Mater.,* 2017, **29**, 8539−8547.

[29] H. Li, P. Wen, Q. Li, C. Dun, J. Xing, C, Lu, S, Adhikari, L. Jiang, D. L. Carroll, S. M. Geyer, Earth-abundant iron diboride (FeB_2) nanoparticles as highly active bifunctional electrocatalysts for overall water splitting, *Adv. Energy. Mater.,* 2017, **7**, 1700513.

[30] J. Wang, H. Zhong, Z. Wang, F. Meng, X. Zhang, Integrated three-dimensional carbon paper/carbon tubes/cobalt-sulfide sheets as an efficient electrode for overall water splitting, *ACS Nano,* 2016, **10**, 2342−2348.

[31] C. Tang, N. Cheng, Z. Pu, W. Xing, X. Sun, NiSe nanowire film supported on nickel foam: an efficient and stable 3D bifunctional electrode for full water splitting, *Angew. Chem., Int. Ed.,* 2015, **54**, 9351–9355.

[32] Y. Li, H. Zhang, M. Jiang, Y. Kuang, X. Sun, X. Duan, Ternary NiCoP nanosheet arrays: an excellent bifunctional catalyst for alkaline overall water splitting, *Nano Res.,* 2016, **9**, 2251–2259.

[33] D. Liu, Q. Lu, Y. Luo, X. Sun, A. M. Asiri, $NiCo_2S_4$ nanowires array as an efficient bifunctional electrocatalyst for full water splitting with superior activity, *Nanoscale,* 2015, **7**, 15122–15126.

[34] W. Chen, H. Wang, Y. Li, Y. Liu, J. Sun, S. Lee, J.-S. Lee, Y. Cui, In situ electrochemical oxidation tuning of transition metal disulfides to oxides for enhanced water oxidation, *ACS Cent. Sci.,* 2015, **1**, 244−251.

[35] J. Yu, Q. Li, N. Chen, C.-Y. Xu, L. Zhen, J. Wu, V. P. Dravid, Carbon-coated nickel phosphide nanosheets as efficient dual-electrocatalyst for overall water splitting, *ACS Appl. Mater. Interfaces,* 2016, **8**, 27850−27858.

[36] L.-A. Stern, L. Feng, F. Song, X. Hu, *Energy Environ. Sci.,* 2015, **8**, 2347–2351.

[37] Z. Peng, D. Jia, A. M. Al-Enizi, A. A. Elzatahry, G. Zheng, Electrocatalysts: from water oxidation to reduction: homologous Ni-Co based nanowires as complementary water splitting electrocatalysts, *Adv. Energy Mater.,* 2015, **5**, 1402031.

[38] D. Li, H. Baydoun, C. N. Verani, S. L. Brock, E□cient water oxidation using CoMnP nanoparticles, *J. Am. Chem. Soc.,* 2016, **138**, 4006–4009.

[39] T. Y. Ma, S. Dai, M. Jaroniec, S. Z. Qiao, Metal-organic framework derived hybrid Co_3O_4-carbon porous nanowire arrays as reversible oxygen evolution electrodes, *J. Am. Chem. Soc.,* 2014, **136**, 13925−13931.

[40] J. Wang, D. Liu, H. Huang, N. Yang, B. Yu, M. Wen, X. Wang, P. K. Chu, X.-F. Yu, In-plane black phosphorus/dicobalt phosphide heterostructure for efficient electrocatalysis, *Angew. Chem., Int. Ed.,* 2018, **57**, 2600–2604.

[41] T. Liu, P. Li, N. Yao, G. Cheng, S. Chen, W. Luo, Y. Yin, CoP-doped MOF-based electrocatalyst for pH-universal hydrogen evolution reaction, *Angew. Chem., Int. Ed.,* 2019, **58**, 4679–4684.

[42] L. Yu, J. Zhang, Y. Dang, J. He, Z. Tobin, P. Kerns, Y. Dou, Y. Jiang, Y. He, S. L. Sui, In situ growth of Ni_2P-Cu_3P bimetallic phosphide with bicontinuous structure on self-supported NiCuC substrate as an efficient hydrogen evolution reaction electrocatalyst, *ACS Catal.,* 2019, **9**, 6919−6928.

[43] K. Fan, H. Chen, Y. Ji, H. Huang, P. M. Claesson, Q. Daniel, B. Philippe, H. Rensmo, F. Li, Y. Luo, L. Sun, Nickel-vanadium monolayer double hydroxide for efficient electrochemical water oxidation, *Nat. Commun.,* 2016, **7**, 11981−11988.

[44] S. Li, Y. Wang, S. Peng, L. Zhang, A. M. Al-Enizi, H. Zhang, X. Sun, G. Zheng, Co-Ni-based nanotubes/nanosheets as efficient water splitting electrocatalysts, *Adv. Energy Mater.,* 2016, **6**, 1501661.

[45] C. Xiao, Y. Li, X. Lu, C. Zhao, Bifunctional porous NiFe/$NiCo_2O_4$/Ni foam electrodes with triple hierarchy and double synergies for efficient whole cell water splitting, *Adv. Funct. Mater.,* 2016, **26**, 3515.

[46] X. Zhao, P. Pachfule, S. Li, J. R. J. Simke, J. Schmidt, A. Thomas, Bifunctional electrocatalysts for overall water splitting from an iron/nickel-based bimetallic

metal-organic framework/dicyandiamide composite, *Angew., Chem. Int. Ed.,* 2018, **57**, 8921–8926.

[47] P. W. Menezes, C. Panda, S. Loos, F. Bunschei-Bruns, C. Walter, M. Schwarze, X. Deng, H. Dau, M. Driess, A structurally versatile nickel phosphite acting as a robust bifunctional electrocatalyst for overall water splitting, *Energy Environ. Sci.,* 2018, **11**, 1287–1298.

[48] H. Sun, Y. Lian, C. Yang, L. Xiong, P. Qi, Q. Mu, X. Zhao, J. Guo, Z. Deng, Y. Peng, A hierarchical nickel-carbon structure templated by metal-organic frameworks for efficient overall water splitting, *Energy Environ. Sci.,* 2018, **11**, 2363–2371.